CHAT

The Colorado Hail Accumulation from Thunderstorms Project

Katja Friedrich, Robinson Wallace, Bernard Meier, Nezette Rydell, Wiebke Deierling, Evan Kalina, Brian Motta, Paul Schlatter, Thomas Schlatter, and Nolan Doesken

The CHAT project aims to collect hail accumulation reports and study the behavior of hail-producing thunderstorms with dual-polarization weather radars and a lightning mapping array.

Hail accumulations at the surface, sometimes up to 50 cm in depth, have occurred frequently enough in metropolitan areas that this phenomenon has caught the attention of the National Weather Service (NWS), the general public, and social/digital media outlets. Motor vehicle accidents, road closures, airport delays, flooding, and swift-water rescues have resulted from hail accumulations on the ground (Fig. 1). A number of these events have occurred across the United States, in particular around the Denver metropolitan area in Colorado, and around the world in previous years (Knight et al. 2008; Schlatter et al. 2008; Schlatter and Doesken 2010; see http://clouds.colorado.edu/deephail). Despite the extreme nature of these storms, adequate reports or measurements of accumulated hail depth are currently not collected or archived, and products to track or forecast these events do not exist, precluding any guidance being issued to emergency responders, transportation departments, and the general public.

To better identify and forecast hail accumulations from thunderstorms, forecasters from the NWS Forecast Office (NWSFO) in Boulder, Colorado, in collaboration with researchers from the University of Colorado Boulder, started the Colorado Hail Accumulation from Thunderstorms (CHAT) project in 2016, which aims to collect hail accumulation reports and study the behavior of hail-producing thunderstorms with dual-polarization weather radars and a lightning mapping array. The CHAT project has four main objectives: i) building a database of reported hail depths, median hail sizes, and hail swath extent; ii) studying typical characteristics of thunderstorms that produce significant hail accumulations on the

AFFILIATIONS: Friedrich and Wallace—Department of Atmospheric and Oceanic Sciences, University of Colorado Boulder, Boulder, Colorado; Meier, Rydell, Motta, and P. Schlatter—NOAA/NWS Forecast Office, Boulder, Colorado; Deierling—Department of Aerospace Engineering, University of Colorado Boulder, and NCAR, Boulder, Colorado; Kalina—University of Colorado Boulder, and Cooperative Institute for Research in Environmental Sciences, NOAA/Earth System Research Laboratory/Global Systems Division, Boulder, Colorado; T. Schlatter*—NOAA/Earth System Research Laboratory/Global Systems Division, Boulder, Colorado; Doesken—Colorado Climate Center, Colorado State University, Fort Collins, Colorado
* Retired.
CORRESPONDING AUTHOR: Katja Friedrich, katja.friedrich@colorado.edu

The abstract for this article can be found in this issue, following the table of contents.
DOI:10.1175/BAMS-D-16-0277.1

In final form 21 August 2018

ground; iii) developing techniques to identify thunderstorms with hail accumulations on the ground using operational weather radar and lightning networks; and iv) developing techniques to nowcast and predict hail accumulation potential on the ground. So far, the CHAT project has focused primarily on storms occurring in eastern Colorado and southeast Wyoming using data from the NWS dual-polarization radar network [Weather Surveillance Radar-1988 Doppler (WSR-88D)] that became available in 2012 and the Colorado Lightning Mapping Array (COLMA) that was installed in northeastern Colorado in the spring of 2012 (Rison et al. 2012). Once results are more robust and algorithms are tested, the project can be expanded to the national level.

Previous research, which focused on hail formation, growth, and decay as well as environmental conditions favoring hail production in convection, has mainly analyzed processes that lead to the growth of hailstones rather than depth of accumulation (e.g., Browning 1964; Browning and Foote 1976; Rasmussen and Pruppacher 1982; Heymsfield 1983; Nelson 1983; Rasmussen and Heymsfield 1987; Miller et al. 1990; Conway and Zrnić 1993; Knight and Knight 2001; Ryzhkov et al. 2013a,b; Grant and van den Heever 2014; Kalina et al. 2014; Dennis and Kumjian 2017). Based on over 50 years of research, Dennis and Kumjian (2017) summarized that maximum hail production can be obtained by hailstones following trajectories through optimal growth environments within thunderstorms. That is, regions between −10° and −25°C with appropriate updraft strength and width and sufficient supercooled water. Additionally, they found that the availability of hail embryos of appropriate size and concentration in locations where they can be advected into the hail growth zones is also important. Storm environmental conditions (e.g., vertical wind shear, buoyancy, vertical profile of humidity, aerosol concentration) have also been identified as important factors for changing storm structure, dynamics, and microphysics, specifically, hail formation and growth (e.g., Weisman and Klemp 1982, 1984; Weisman and Rotunno 2000; van den Heever and Cotton 2004; Dennis and Kumjian 2017).

Much of the research on identifying and forecasting the growth of large hailstones has been implemented into algorithms and procedures used by the NWS. Currently, the NWS issues a severe thunderstorm warning when a thunderstorm is expected to produce hail ≥2.5 cm (1 in.) in diameter. Over the last decade, NWS has sought to increase the number of maximum hail size reports through social media, NWS storm reports (also referred to as *Storm Data*), or multiyear field campaigns. It has also evaluated the quality of these reports (e.g., Dobur 2005; Doswell et al. 2005; Ashley et al. 2008; Cecil 2009; Ortega et al. 2009; Blair and Leighton 2012; Blair et al. 2017). Even so, reliable and detailed reports of accumulated hail depth, median hail size, and hail swath extent remain rare.

Kalina et al. (2016) performed one of the first comprehensive studies that analyzed synoptic conditions and radar and lighting signatures of four thunderstorms along the Front Range, each with >15 cm of hail accumulation at the surface. Though these events were associated with slow storm motion (6–9 m s^{-1}), the radar and lightning signatures of these hail events were not substantively different

Fig. 1. Photograph of hail accumulation in Lakewood, CO, after the 9 Sep 2013 hailstorm. (Reprinted with permission from www.thedenverchannel.com/news/hail-rain-pours-in-lakewood-wheat-ridge. Photo credit: 7NEWS reporter Marshall Zelinger.)

from what has been observed in other severe hailstorms without hail accumulations. Nevertheless, Kalina et al. (2016) found that hail accumulations are associated with large hail production or presence in the cloud and slow storm propagation speeds or a combination of these. Continuing the work by Kalina et al. (2016), Wallace et al. (2019) used 20 reliable hail depth reports along the Front Range to refine a radar-based hail accumulation algorithm that was the basis of the Kalina et al. (2016) study. Wallace et al. (2019) validated this revised algorithm with a larger dataset of 32 thunderstorms and showed that the ratio between reported and radar-based hail accumulations at the time and location of the report ranged between 0.6 and 1.5 for 80% of the reports where >3 cm of hail accumulations was observed on the ground. Other NWSFOs such as Amarillo, Texas, have also started to use dual-polarization weather radar information to identify thunderstorms with hail accumulations (Ward et al. 2018).

This article highlights the importance of observing and reporting hail depth and the need to bring forward new ideas and state-of-the-art practices for identifying, tracking, and nowcasting surface hail accumulations from thunderstorms. It highlights some of the first results and lists remaining challenges.

HIGHLIGHTS AND FIRST RESULTS. *Building a hail depth database*. For the period of study, 2012–17, we collected hail depth information from storm reports complied by the NWS (*Storm Data*) and the Community Collaborative Rain, Hail and Snow (CoCoRaHS; see www.cocorahs.org/; Reges et al. 2016) network or reported in newspapers and by broadcast media. Since hail depth is currently not required for hail reporting, we have asked amateur meteorologists and storm spotters since 2016 to send texts, photos, video, and drone footage of hail depth, hail size distribution, and hail swath extent using Facebook, Twitter, telephone, or e-mail (Fig. 2a). Figure 2b shows a sample report submitted from the field. A total of 91 hail depth reports were collected from 60 thunderstorms in the study area from 2012 through 2017 (Fig. 3); 64% of the reports were from 2016. So far, we have analyzed 32 storms (52 reports) that occurred within the COLMA and the range of the operational dual-polarization radars in Pueblo, Colorado; Denver; and Cheyenne, Wyoming, and that passed our quality control criteria. For a report to be included in the analysis, it had to meet the following requirements: i) the report had to include the precise location of the event, ii) the location had to be within 150 km of a Next Generation Weather Radar (NEXRAD), iii) precipitation had to be detected by the radar at the location of the report between the time of the report and 1 h prior, and iv) if the report was transmitted via social media, it had to be accompanied by a picture to verify the reported hail depth. For more information on quality control criteria, we refer the reader to Wallace et al. (2019).

The quality of the reports varies greatly depending on the source. Overviews of how social media information can be included in hail observation datasets are given, for example, by Hyvärinen and Saltikoff (2010), Blair and Leighton (2012), Allen and Tippett (2015), and Brimelow and Taylor (2017). Unfortunately, out of the 60 thunderstorms (91 reports), 28 storms (59 reports) could not be analyzed

Fig. 2. Hail depth reporting as part of the CHAT project: (a) 2018 flyer with detailed information sent out by the NWS and (b) Twitter response for hail accumulations on 29 Aug 2016. For more information on how and where to submit reports, please visit our website at http://clouds.colorado.edu/deephail. [Photo credit for (b): CBS4 reporter Rob McClure.]

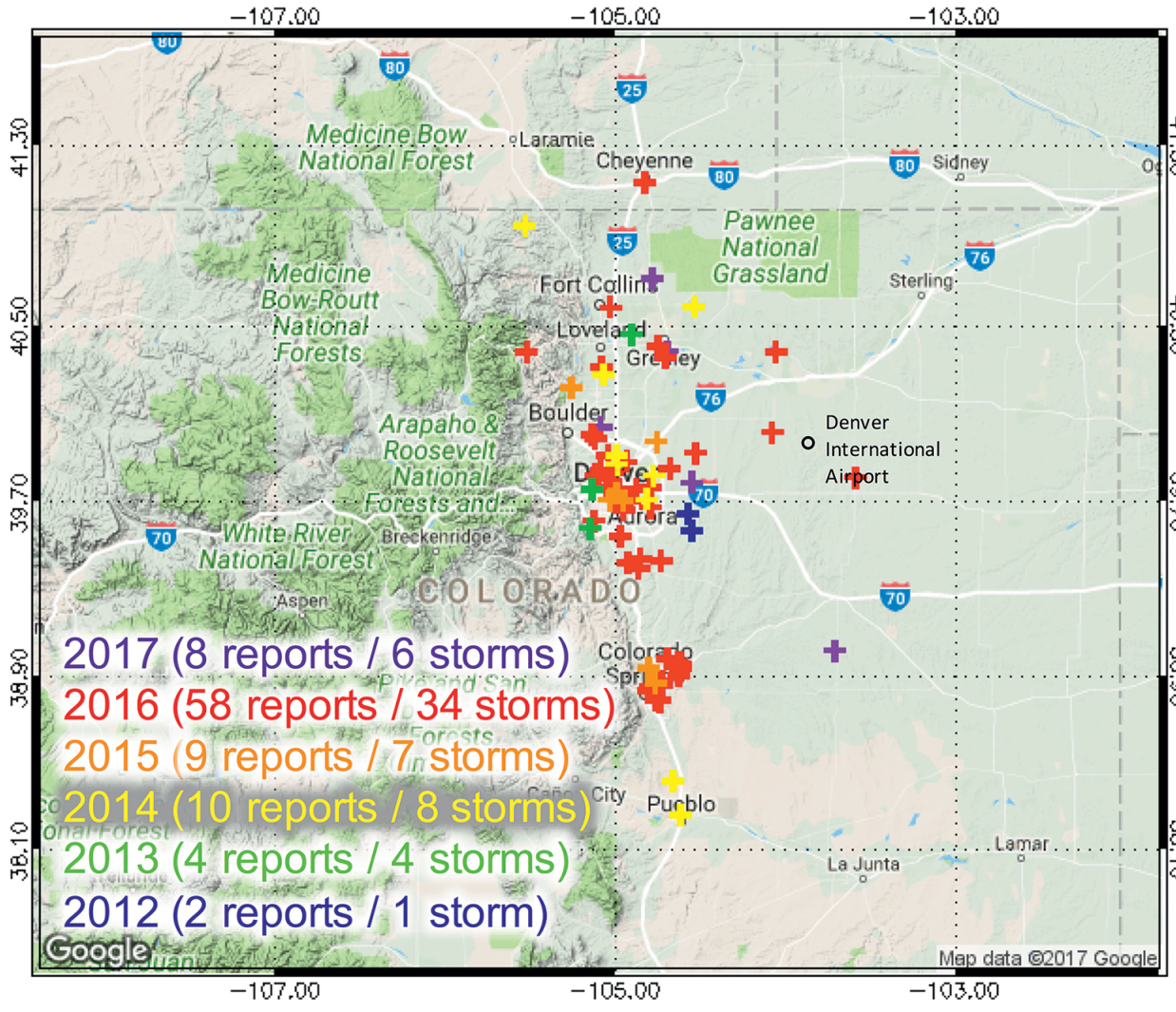

Fig. 3. Archived reports of hail accumulations from thunderstorms along the Colorado Front Range between 2012 and 2017 (color coded). The number of reports for each year is listed in parentheses. Sources include CoCoRaHS reports, NWS storm reports (*Storm Data*), Twitter, Facebook, news outlets, and trained spotters.

because they did not satisfy the quality control criteria. Of the 32 analyzed thunderstorms, 14 had traces of hail or accumulations under 3 cm (trace or small; see Fig. 7 in Wallace et al. 2019), 9 had accumulations between 3 and 10 cm (moderate), and 9 had more than 10 cm of hail accumulation (deep).

Identifying thunderstorms producing hail accumulations on the ground. Though hail depth reports are crucial in determining which thunderstorms produce moderate-to-deep hail accumulations, more information is needed. To remedy this, Kalina et al. (2016) used radar reflectivity and a radar-based hydrometeor classification to estimate surface hail accumulations. Wallace et al. (2019) improved upon this by including information on maximum hail size from the radar-based maximum estimated size of hail (MESH) algorithm (Witt et al. 1998) to derive maximum fall velocity using the diameter–fall velocity relationship for rimed particles from Heymsfield and Wright (2014). Validating this revised algorithm against 20 high-quality hail depth reports resulted in a correlation coefficient between radar-based and reported hail accumulations of 0.88, an improvement from the value of 0.69 obtained by Kalina et al. (see Fig. 8 in Wallace et al. 2019).

Two examples of radar-based hail accumulations using the validated algorithm in Wallace et al. (2019) are shown in Fig. 4. One example shows a series of multicell thunderstorms that occurred on 28–29 June 2016, which started to accumulate hail ~20 km northwest of Denver, moving southeast at a speed of about 12 m s^{-1} (Fig. 4a). We received three hail depth reports on that day in or close to the areas of deepest

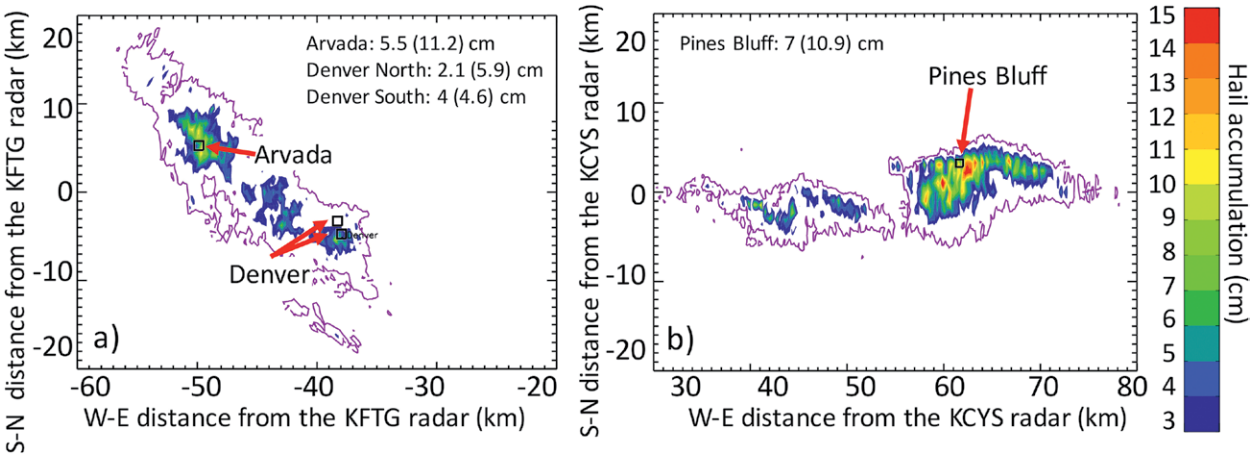

Fig. 4. Radar-based total hail accumulations (a) between 2300 UTC 28 Jun and 0100 UTC 29 Jun and (b) between 2230 and 2359 UTC 27 Jul 2016 with report locations indicated by red arrows and small black squares. Radar data from WSR-88Ds at (a) Denver (KFTG) and (b) Cheyenne (KCYS) were used for this analysis. Hail accumulations between 1 and <3 cm are outlined by the magenta contours. Reported hail depths are listed with radar-based accumulations in parentheses.

accumulations indicated by the radar. Differences between reported and radar-derived accumulations ranged between 0.6 and 3.8 cm around Denver and 5.7 cm at Arvada, Colorado. The second example shows a supercell thunderstorm first observed about 30 km east of Cheyenne. It moved east at 8 m s^{-1} during the accumulation period. A 7-cm accumulation was reported along Interstate Highway 80 (I-80) close to Pines Bluff, Wyoming, while radar indicated a hail accumulation of about 11 cm. From Fig. 4, the ratios between the reported and radar-based hail accumulations are 0.49, 0.35, 0.87, and 0.64. This compares fairly well with the range of ratios from 0.6 to 1.5, quoted earlier from Wallace et al. (2019), for 80% of 32 hail depth reports.

From this point on we analyze the temporal and spatial evolution of lightning and radar variables using the validated radar-based hail accumulations along the Colorado and southern Wyoming Front Range. Radar-based hail accumulations together with the variables discussed in this paper are also calculated in real time during the convective seasons for eastern Colorado, near Rapid City, South Dakota, and Amarillo (http://clouds.colorado.edu/Real-timeHailMaps). This preliminary nowcasting product is currently tested by the Boulder NWSFO and results are used for further research. We anticipate further validation of the radar-based hail depth algorithm as we receive more reports but also would like to test the algorithm in other areas first. Thus, we wish to solicit hail depth reports across the entire United States. For more information on how to submit reports, visit our website (http://clouds.colorado.edu/deephail) or reach us (@DeepHailCO) or our local weather forecast office on Twitter (e.g., @NWSBoulder, #deephail).

We also track several additional lightning variables associated with hailstorms. These include lightning flash rate and flash extent density. The former refers to the number of flash initiation points in over an area of 1 km × 1 km, and the latter is the number of flashes that cross a vertical column with a cross section of 1 km^2 in 1 min (Bruning and MacGorman 2013; Mansell 2014). These variables are both derived from Lightning Mapping Array measurements and are linked to storm updraft strength, updraft volume, and graupel mass (e.g., Carey and Rutledge 2000; Wiens 2005; Wiens et al. 2005; Tessendorf et al. 2007; Deierling and Petersen 2008; Deierling et al. 2008). Numerous studies have shown that increases in lightning flash rate precede hailfall by 5–20 min (e.g., Williams et al. 1999; Goodman et al. 2005; Wiens et al. 2005; Schultz et al. 2009; Darden et al. 2010; Rudlosky and Fuelberg 2013; Schultz et al. 2015). For the two examples shown in Fig. 4, enhanced flash extent density was observed in the vicinity of the deepest accumulations (Figs. 5a,b). On 28–29 June, flash extent density peaked at 2.5 flashes km^{-2} min^{-1} east of Denver and on 27 July a maximum of 3.5–4.0 flashes km^{-2} min^{-1} was observed over the area of maximum observed hail accumulation, east and south of Pines Bluff. For flash extent density, we found that the changes are typically more important than the specific values for determining hail potential.

As part of the real-time hail accumulation maps, we track vertically integrated ice (VII; Figs. 5c,d), which integrates radar reflectivity >35 dBZ at

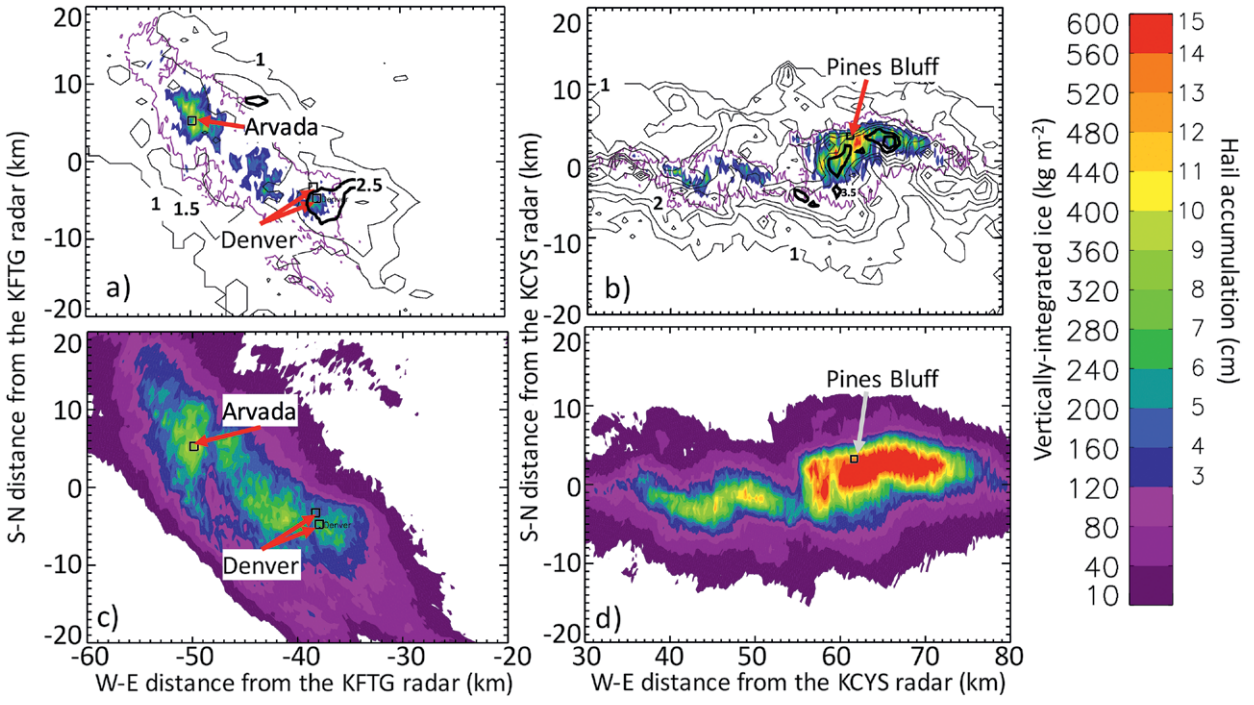

Fig. 5. Radar-based (top) total hail accumulation (color coded) as in Figs. 4a and 4b overlaid with flash extent density and (bottom) VII. All variables are accumulated (a),(c) between 2300 UTC 28 Jun and 0100 UTC 29 Jun and (b),(d) between 2230 and 2345 UTC 27 Jul 2016. Red or white arrows point to reports. Radar data from WSR-88Ds at (a),(c) Denver and (b),(d) Cheyenne were used for this analysis. In (a) and (b), the flash extent density contours start at 1 flash km^{-2} min^{-1}. The contour interval is 0.5 flashes km^{-2} min^{-1}. Enhanced areas of flash extent density are enclosed by thick black contours at 2.5 km^{-2} min^{-1} in (a) and (b).

altitudes where the temperature ranges from −10° to −40°C and converts it into VII following the method described in Carey and Rutledge (2000), Gauthier et al. (2006), and Mosier et al. (2011). Enhanced VII is often observed upstream or in the area of moderate-to-deep hail accumulations. Figure 5 bears this out. In the next section, we show how VII and storm speed are linked to hail accumulation by analyzing the 32 thunderstorms in our database.

Studying characteristics of thunderstorms producing hail accumulations on the ground. Most of the moderate (3–10 cm) and deep (>10 cm) hail accumulations were observed in supercell thunderstorms (Fig. 6). An analysis of the operational sounding closest in time (mostly at 0000 UTC) and space (approximately 50–180 km) to the hail report of the 32 storms included in our study showed that for the moderate and deep hail accumulations wind speeds averaged between 0 and 6 km AGL are 4 m s^{-1} less; column-integrated precipitable water vapor averages are 4 mm larger, and 0–6-km wind shear is 5 m s^{-1} larger compared to proximity soundings when thunderstorms produced <3 cm of hail.

Intuition suggests that slow-moving storms might favor deeper hail accumulations. However, the analysis of 32 storms shows that storms propagating at >16 m s^{-1} (large circles in Fig. 7) can still produce maximum hail accumulations >10 cm (orange and red circles in Fig. 7), whereas slow-moving storms of <7 m s^{-1} (small circles) can cause trace, moderate, or deep accumulations. Combining a measure of cloud ice with storm speed might provide a better way to estimate hail accumulation. Hence, we use maximum VII (Figs. 5c,d) every 5 min and then average it over the time hail was identified at the surface using the NWS radar particle identification (PID) algorithm (Park et al. 2009). To calculate hail accumulations in real time, storm speed was derived from the level III product available from the operational radars. Note that the hail accumulations presented in Fig. 7 are radar based. As noted earlier, Wallace et al. (2019) showed that the correlation coefficient between hail depth reports and radar-derived accumulations is about 0.87 and that the ratio between the two is within 0.66–1.5 for 80% of the cases with accumulations >3 cm. The study was based on 20 high-quality reports, which are part of the 32 thunderstorms shown in Fig. 7.

The relationship between hail accumulation and time-averaged maximum VII leads to clustering into three main groups: i) storms with low VII

of <50 kg m^{-2} produced <3 cm of accumulated hail and had low accumulation rates of <0.4 cm min^{-1}; ii) storms with moderate VII between 50 and 150 kg m^{-2} produced moderate-to-deep hail accumulations and had moderate-to-fast (0.4–0.9 cm min^{-1}) time-averaged accumulation rates, depending on the storm speed; and iii) storms with large VII of >150 kg m^{-2} produced deep hail (>10 cm) and accumulation rates of 0.9–2.5 cm min^{-1}. (One storm in the third cluster had a VII of only 130 kg m^{-2} but the accumulation rate was still 1.2 cm min^{-1}.) Storms that produce copious hail (orange and red circles in Fig. 7) move at a variety of speeds (5–14 m s^{-1}), but clearly do not produce intense hailfall at every moment of their existence. However, a comparison of all cases with copious hail (orange and red circles in Fig. 7) indicates that slowly moving thunderstorms with lower VII (three red circles with VII of ~100 kg m^{-2}) dropped as much hail as faster-moving thunderstorms with higher VII (four red circles with VII of 130–220 kg m^{-2}). Thus, in some cases hail accumulation depends upon storm speed, VII, and hail core size. Storms with lower VII (~50–150 kg m^{-2}) have to move more slowly or need to have a wider hail core to produce significant accumulations on the ground. Storms with the highest VII (>150 kg m^{-2}) tend to deliver hail at the ground at the highest accumulation rates; in general, slower-moving storms accumulate more hail than faster-moving storms.

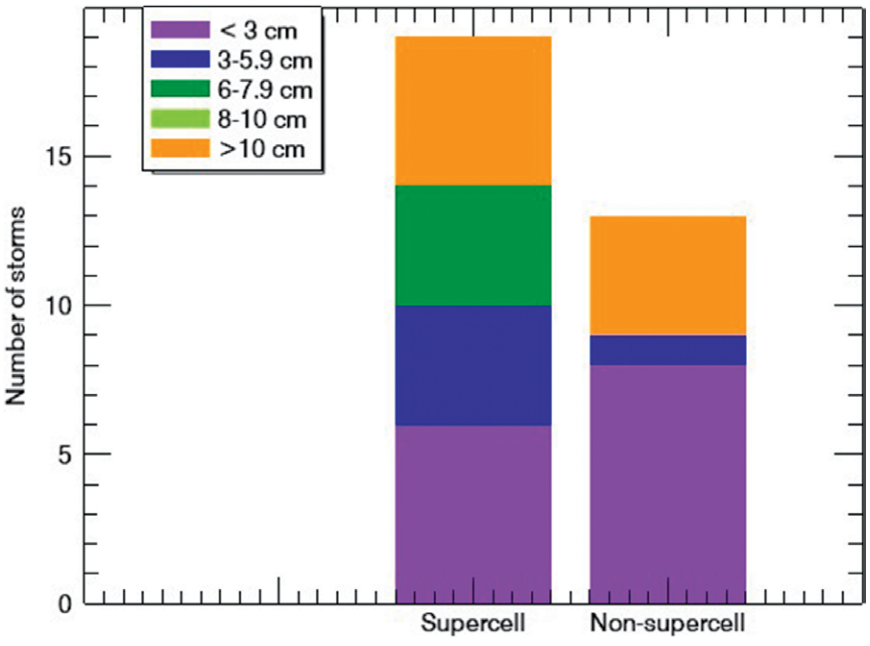

Fig. 6. Classification of 32 thunderstorms analyzed in this study as a function of maximum radar-based hail accumulation depth for each event.

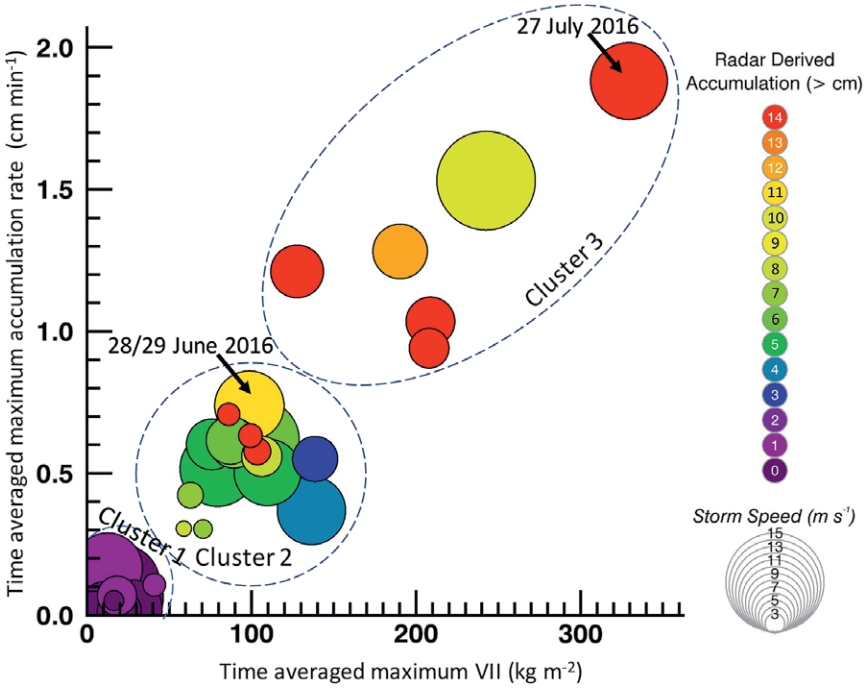

Fig. 7. Time-averaged maximum hail accumulation rate as a function of time-averaged maximum VII for the thunderstorms included in our study. Hail accumulations were derived from the radar-based hail accumulation maps for each event. Bubble size indicates mean storm speed derived from radar echo motion; color indicates maximum hail accumulation of the entire storm. Hailfall durations ranged from 5 to 25 min with hail swaths from a few hundred meters to a kilometer wide. Dashed lines enclose three clusters of storms discussed in the text; two cases discussed in the text are also highlighted.

We have analyzed a variety of other dual-polarization radar, radar-derived,

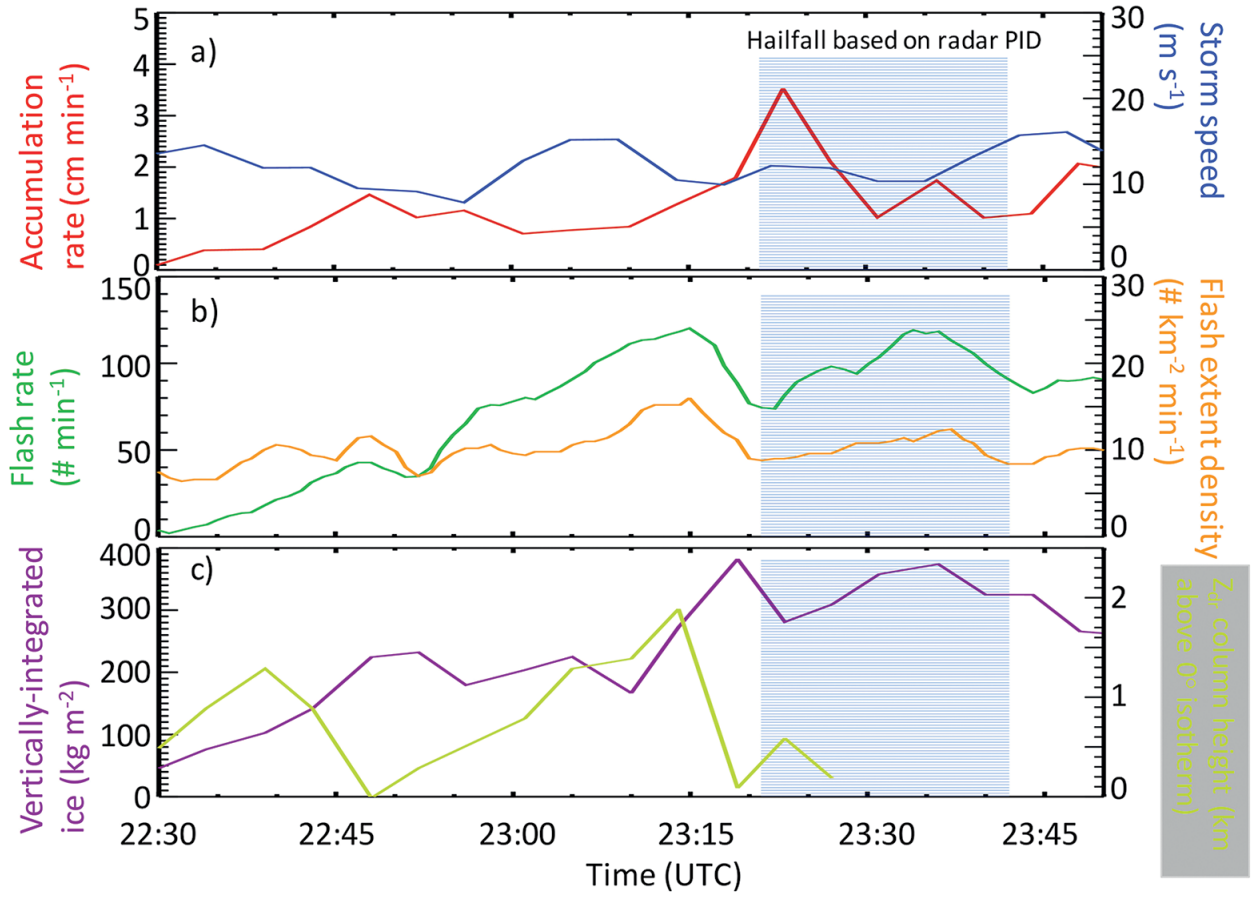

Fig. 8. Temporal evolution of hail-related parameters for the Pines Bluff storm on 27 Jul 2016: (a) mean accumulation rate (red line) and storm speed (blue line) based on 5-min radar data, (b) flash rate (green line) and flash extent density (orange line) based on 1-min lightning data, and (c) VII (purple line) and the height of the positive Z_{dr} column above the 0°C isotherm (light green line) based on 5-min radar data. Time interval when the radar PID scheme identified hail falling over the reported locations is indicated by the blue horizontal lines.

and lightning variables as shown in Kalina et al. (2016) to estimate hail growth and melting rates. The computation of some variables is not yet possible in real time, which diminishes their utility. Moreover, correlations among some of these variables and hail accumulation are not particularly strong. For instance, specific differential phase K_{dp}, the change in the phase difference between horizontally and vertically polarized waves, measured along the beam, is a good indicator of large amounts of water in the cloud. Occasionally, but not always, K_{dp} exceeds 6° km^{-1} prior to or during hailfall, indicating that rain is mixed with water-coated hailstones (Kalina et al. 2016). Peaks in lightning flash rate have been observed at or near the location of hailfall but so far cannot be used reliably to estimate the depth and location of moderate and deep hail accumulations (Kalina et al. 2016). A bounded weak-echo region, an indicator for the location and strength of the main updraft and an area of hydrometeor recycling, has sometimes been observed about 5 min prior to hailfall. However, evidence suggests that it is neither a necessary nor sufficient feature for hail production (Knight 1984; Kalina et al. 2016). The differential radar reflectivity Z_{dr} is the difference in returned energy between the horizontally and vertically polarized pulses. Positive values of Z_{dr} above the freezing level indicate large supercooled liquid drops lofted by the updraft to great heights before freezing (Kumjian et al. 2014). The height of these positive Z_{dr} columns has been used as a proxy for updraft strength. We identified these Z_{dr} columns in some of the thunderstorms prior to hailfall but, again, doing so in real time remains challenging.

Identifying thunderstorms producing hail accumulations on the ground. We wondered if the temporal evolution of hail-related variables might provide some guidance for nowcasting hail accumulation potential. We present here the temporal evolution of selected radar

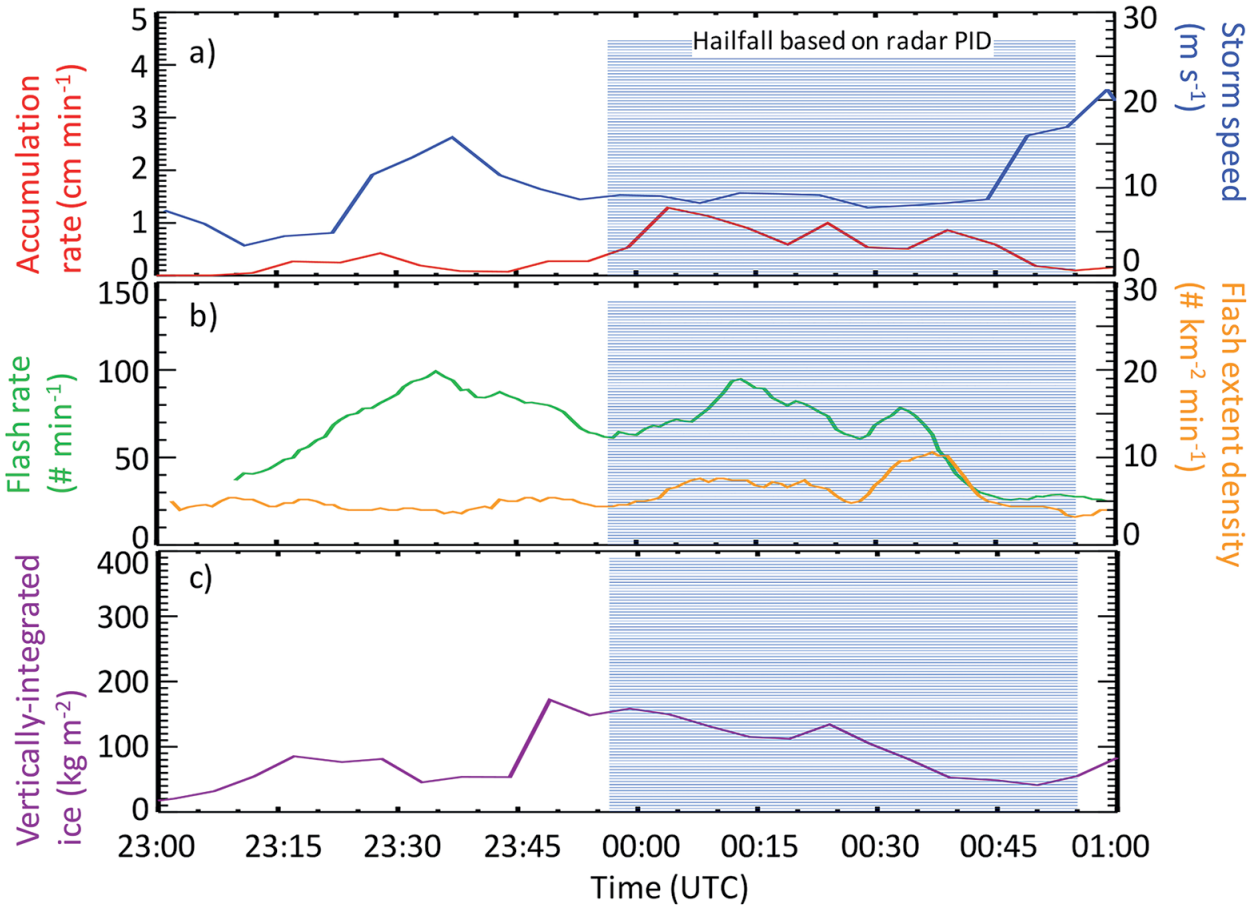

Fig. 9. As in Fig. 8, but for the Denver–Arvada hailstorm on 28–29 Jun 2016. A positive Z_{dr} column was not detected from the radar data and, therefore, is not shown in (c).

and lightning variables for the two storms previously discussed to demonstrate the challenges in predicting accumulations even minutes ahead of time.

Figure 8 shows a selection of radar and lightning variables for the Pines Bluff hailstorm on 27 July 2016. The actual hail depth (7 cm) was derived from a webcam along I-80, which indicated no measurable accumulation after 2330 UTC. The corresponding radar-based estimate of hail accumulation was 10.9 cm. Based on the webcam, most of the hail accumulated over a 3-min period prior to 2330 UTC. The radar-estimated hail accumulation rate peaked at 3.5 cm min^{-1} (Fig. 8a). This occurred during the period of hailfall (blue shading in Fig. 8a), as inferred from the PID scheme mentioned above. At 4–9 min prior to the maximum accumulation rate, the flash rate and the flash extent density peaked (Fig. 8b), as did the VII and the height of the positive Z_{dr} column above the freezing level (Fig. 8c). Sudden increases or so-called jumps in flash rate have been associated with increased hail production (Schultz 2015; Schultz et al. 2015). The storm speed remained between 12 and 18 m s^{-1} (Fig. 8a), but the storm slowed slightly prior to hailfall. Note that storms with similar deep hail accumulations (>14 cm of total accumulations) had in general lower storms speeds with 3–7 m s^{-1} (Fig. 7; Kalina et al. 2016).

Similar patterns of behavior were noted for the Denver–Arvada hailstorm on 28–29 June 2016 (Fig. 9). The three maxima in accumulation rate (Fig. 9a) correspond approximately to the three areas of enhanced hail accumulation in Fig. 4a, with one report from the first accumulation period (around 0005 UTC) and two reports from the third accumulation period (around 0040 UTC). The maximum accumulation rates of 0.8–1.3 cm min^{-1} are much smaller than on 27 July and therefore resulted in much smaller accumulations (Fig. 4a). Peaks in VII (Fig. 9c) prior to peaks in accumulation rates (Fig. 9a) are only observed for the first and third maxima. However, the third maximum in accumulation rate also shows an increase in flash extent density ~5 min prior and flash rate ~7 min prior (Fig. 9b). The second maximum in accumulation rate might be related to

the increase in flash rate ~15 min earlier. The storm slowed down slightly from 12 to 8 m s^{-1} (Fig. 9a) prior to hailfall and sped up to 22 m s^{-1} toward the end of hailfall at 0045 UTC. We were unable to detect the positive Z_{dr} columns of the storm.

We have analyzed the radar and lightning variables discussed above for all 32 thunderstorms. In summary, a maximum in VII has been consistently observed 5–20 min prior to the first maximum of the radar-based accumulation rate associated with hailfall, while the temporal evolution of other lightning and radar variables varies from case to case. Because VII and hail accumulations were both derived from radar data, the variables are not necessarily independent. Many questions remain to be answered regarding lightning activity and hail accumulation potential. Automating the computation of these variables throughout the lifetime of the storm and comparing them with the two-dimensional maps will be a first step toward a nowcasting algorithm for better estimating the time and location of deep hailfall.

LESSIONS LEARNED AND FUTURE STEPS.

Hail accumulations from thunderstorms affect thousands of people and pose hazards to life and property. No comprehensive reports, measurement standards, or forecasts of accumulated hail depth, hail size distributions, and hail swath extent are currently in place. The Colorado Hail Accumulation from Thunderstorms (CHAT) project aims to address some of these shortcomings by improving the frequency, accuracy, and information content of hail reports, thereby defining the "possibly" unique characteristics of storms that produce copious amounts of hail, and identifying useful predictors to be utilized for nowcasting purposes. Detailed analyses are currently under way, but preliminary guidance for identifying and estimating hail accumulation at the surface can be summarized as follows:

- It is vital to rethink hail reporting because it is fundamental for studying hail accumulations in thunderstorms and also for verifying radar-based estimates of hail accumulation are high-quality reports of hail depth, hail swath extent, and hail size distribution in an operational reporting system. Various hail depth reporting systems have already been implemented in the standard reporting programs, including in operational NWS storm reporting and CoCoRaHS. Thus far, Twitter has been the most efficient way to report hail depth, including pictures and videos, yet many of the reports are imprecise or incomplete regarding time, duration, and location. Moreover, information on hail swath extent and hail size distribution is rare.
- Preliminary results indicate that radar-derived hail accumulation maps show promise in identifying hail swath extent and quantity of hail accumulations along the Colorado–Wyoming Front Range. More direct measurements are needed to better verify their accuracy within the study area and beyond.
- To work toward a nowcasting algorithm, we need to track hail production and its presence in clouds, and also consider environmental conditions, including storm speed, that affect hail production and duration and melting of hailstones.

The goal of future research is to improve our basic knowledge about the evolution of radar and lightning characteristics of thunderstorms producing copious hail. We are working to include more cases from Colorado and elsewhere to provide more robust statistics and results that can be implemented into a nowcasting algorithm. We plan to investigate the role of terrain-induced boundaries and thunderstorm outflow boundaries on the rapid intensification of thunderstorms as well as the effect of melting on hailstones below the freezing level. Surface boundary interactions affected several thunderstorms in our dataset and may have influenced hail accumulations. Finally, we want to take advantage of new measurement technologies on board *Geostationary Operational Environmental Satellite-16* (*GOES-16*). Images at 30- and 60-s intervals and total lightning data will be a boon, especially in data-sparse areas, for revealing storm-scale boundaries, circulations, and the locations of hail swaths in real time. However, the ultimate goal is to *predict* hail accumulations from thunderstorms either through a nowcasting system or with numerical weather prediction models.

ACKNOWLEDGMENTS. We thank all volunteers who have reported hail depth and all volunteers who have participated in the CHAT project. Thanks go to Brielle Kissack and Bailey Donaldson of the University of Colorado for compiling some of the hail depth reports. Some of this material is based upon work supported by the COMET GOES-R Partners Project under the UCAR Award Z16-23464 and under National Science Foundation Grant AGS-1555540. Extensive feedback from three anonymous reviewers greatly improved earlier versions of this manuscript.

REFERENCES

Allen, J. T., and M. K. Tippett, 2015: The characteristics of United States hail reports: 1955–2014. *Electron. J. Severe Storms Meteor.*, **10** (3), www.ejssm.org/ojs/index.php/ejssm/article/viewArticle/149.

Ashley, W. S., A. J. Krmenec, and R. Schwantes, 2008: Vulnerability due to nocturnal tornadoes. *Wea. Forecasting*, **23**, 795–807, https://doi.org/10.1175/2008WAF2222132.1.

Blair, S. F., and J. W. Leighton, 2012: Creating high-resolution hail datasets using social media and post-storm ground surveys. *Electron. J. Oper. Meteor.*, **13**, 32–45, http://nwafiles.nwas.org/ej/pdf/2012-EJ3.pdf.

——, and Coauthors, 2017: High-resolution hail observations: Implications for NWS warning operations. *Wea. Forecasting*, **32**, 1101–1119, https://doi.org/10.1175/WAF-D-16-0203.1.

Brimelow, J. C., and N. M. Taylor, 2017: Verification of the MESH product over the Canadian prairies using a high-quality surface hail report dataset sourced from social media. *38th Conf. on Radar Meteorology*, Chicago, IL, Amer. Meteor. Soc., 240, https://ams.confex.com/ams/38RADAR/webprogram/Paper321272.html.

Browning, K. A., 1964: Airflow and precipitation trajectories with severe local storms which travel to the right of the winds. *J. Atmos. Sci.*, **21**, 634–639, https://doi.org/10.1175/1520-0469(1964)021<0634:AAPTWS>2.0.CO;2.

——, and G. B. Foote, 1976: Airflow and hail growth in supercell storms and some implications for hail suppression. *Quart. J. Roy. Meteor. Soc.*, **102**, 499–533, https://doi.org/10.1002/qj.49710243303.

Bruning, E. C., and D. R. MacGorman, 2013: Theory and observations of controls on lightning flash size spectra. *J. Atmos. Sci.*, **70**, 4012–4029, https://doi.org/10.1175/JAS-D-12-0289.1.

Carey, L. D., and S. A. Rutledge, 2000: The relationship between precipitation and lightning in tropical island convection: A C-band polarimetric study. *Mon. Wea. Rev.*, **128**, 2687–2710, https://doi.org/10.1175/1520-0493(2000)128<2687:TRBPAL>2.0.CO;2.

Cecil, D. J., 2009: Passive microwave brightness temperatures as proxies for hailstorms. *J. Appl. Meteor. Climatol.*, **48**, 1281–1286, https://doi.org/10.1175/2009JAMC2125.1.

Conway, J. W., and D. S. Zrnić, 1993: A study of embryo production and hail growth using dual-Doppler and multiparameter radars. *Mon. Wea. Rev.*, **121**, 2511–2528, https://doi.org/10.1175/1520-0493(1993)121<2511:ASOEPA>2.0.CO;2.

Darden, C. B., D. J. Nadler, B. C. Carcione, R. J. Blakeslee, G. T. Stano, and D. E. Buechler, 2010: Utilizing total lightning information to diagnose convective trends. *Bull. Amer. Meteor. Soc.*, **91**, 167–175, https://doi.org/10.1175/2009BAMS2808.1.

Deierling, W., and W. A. Petersen, 2008: Total lightning activity as an indicator of updraft characteristics. *J. Geophys. Res.*, **113**, D16210, https://doi.org/10.1029/2007JD009598.

——, ——, J. Latham, S. Ellis, and H. J. Christian, 2008: The relationship between lightning activity and ice fluxes in thunderstorms. *J. Geophys. Res.*, **113**, D15210, https://doi.org/10.1029/2007JD009700.

Dennis, E. J., and M. R. Kumjian, 2017: The impact of vertical wind shear on hail growth in simulated supercells. *J. Atmos. Sci.*, **74**, 641–663, https://doi.org/10.1175/JAS-D-16-0066.1.

Dobur, J. C., 2005: A comparison of severe thunderstorm warning verification statistics and population density within the NWS Atlanta county warning area. Preprints, *Fourth Annual Severe Storms Symp.*, Starkville, MS, East Mississippi Chapter, National Weather Association, D2–6, www.weather.gov/media/ffc/SEconf.pdf.

Doswell, C. A., III, H. E. Brooks, and M. P. Kay, 2005: Climatological estimates of daily local nontornadic severe thunderstorm probability for the United States. *Wea. Forecasting*, **20**, 577–595, https://doi.org/10.1175/WAF866.1.

Gauthier, M. L., W. A. Petersen, L. D. Carey, and H. J. Christian Jr., 2006: Relationship between cloud-to-ground lightning and precipitation ice mass: A radar study over Houston. *Geophys. Res. Lett.*, **33**, L20803, https://doi.org/10.1029/2006GL027244.

Goodman, S. J., and Coauthors, 2005: The North Alabama Lightning Mapping Array: Recent severe storm observations and future prospects. *Atmos. Res.*, **76**, 423–437, https://doi.org/10.1016/j.atmosres.2004.11.035.

Grant, L. D., and S. C. van den Heever, 2014: Microphysical and dynamical characteristics of low-precipitation and classic supercells. *J. Atmos. Sci.*, **71**, 2604–2624, https://doi.org/10.1175/JAS-D-13-0261.1.

Heymsfield, A. J., 1983: Case study of a hailstorm in Colorado. Part IV: Graupel and hail growth mechanisms deduced through particle trajectory calculations. *J. Atmos. Sci.*, **40**, 1482–1509, https://doi.org/10.1175/1520-0469(1983)040<1482:CSOAHI>2.0.CO;2.

——, and R. Wright, 2014: Graupel and hail terminal velocities: Does a "supercritical" Reynolds number apply? *J. Atmos. Sci.*, **71**, 3392–3403, https://doi.org/10.1175/JAS-D-14-0034.1.

Hyvärinen, O., and E. Saltikoff, 2010: Social media as a source of meteorological observations.

Mon. Wea. Rev., **138**, 3175–3184, https://doi.org/10.1175/2010MWR3270.1.

Kalina, E. A., K. Friedrich, H. Morrison, and G. H. Bryan, 2014: Aerosol effects on idealized supercell thunderstorms in different environments. *J. Atmos. Sci.*, **71**, 4558–4580, https://doi.org/10.1175/JAS-D-14-0037.1.

——, ——, B. C. Motta, W. Deierling, G. T. Stano, and N. N. Rydell, 2016: Colorado plowable hailstorms: Synoptic weather, radar, and lighting characteristics. *Wea. Forecasting*, **31**, 663–693, https://doi.org/10.1175/WAF-D-15-0037.1.

Knight, C. A., 1984: Radar and other observations of two vaulted storms in northeastern Colorado. *J. Atmos. Sci.*, **41**, 258–271, https://doi.org/10.1175/1520-0469(1984)041<0258:RAOOOT>2.0.CO;2.

——, and N. C. Knight, 2001: Hailstorms in severe convective storms. *Severe Convective Storms*, *Meteor. Monogr.*, Vol. 50, Amer. Meteor. Soc., 223–254.

——, P. T. Schlatter, and T. W. Schlatter, 2008: An unusual hailstorm on 24 June 2006 in Boulder, Colorado. Part II: Low-density growth of hail. *Mon. Wea. Rev.*, **136**, 2833–2848, https://doi.org/10.1175/2008MWR2338.1.

Kumjian, M. R., A. P. Khain, N. Benmoshe, E. Ilotoviz, A. V. Ryzhkov, and V. T. Phillips, 2014: The anatomy and physics of *Z*DR columns: Investigating a polarimetric radar signature with a spectral bin microphysical model. *J. Appl. Meteor. Climatol.*, **53**, 1820–1843, https://doi.org/10.1175/JAMC-D-13-0354.1.

Mansell, E. R., 2014: Storm-scale ensemble Kalman filter assimilation of total lightning flash-extent data. *Mon. Wea. Rev.*, **142**, 3683–3695, https://doi.org/10.1175/MWR-D-14-00061.1.

Miller, L. J., J. C. Fankhauser, and G. B. Foote, 1990: Precipitation production in a large Montana hailstorm: Airflow and particle growth trajectories. *J. Atmos. Sci.*, **47**, 1619–1646, https://doi.org/10.1175/1520-0469(1990)047<1619:PPIALM>2.0.CO;2.

Mosier, R. M., C. Schumacher, R. E. Orville, and L. D. Carey, 2011: Radar nowcasting of cloud-to-ground lightning over Houston, Texas. *Wea. Forecasting*, **26**, 200–212, https://doi.org/10.1175/2010WAF2222431.1.

Nelson, S. P., 1983: The influence of storm flow structure on hail growth. *J. Atmos. Sci.*, **40**, 1965–1983, https://doi.org/10.1175/1520-0469(1983)040<1965:TIOSFS>2.0.CO;2.

Ortega, K. L., T. M. Smith, K. L. Manross, A. G. Kolodziej, K. A. Scharfenberg, A. Witt, and J. J. Gourley, 2009: The Severe Hazards Analysis and Verification Experiment. *Bull. Amer. Meteor. Soc.*, **90**, 1519–1530, https://doi.org/10.1175/2009BAMS2815.1.

Park, H. S., A. V. Ryzhkov, D. S. Zrnić, and K. Kim, 2009: The hydrometeor classification algorithm for the polarimetric WSR-88D: Description and application to an MCS. *Wea. Forecasting*, **24**, 730–748, https://doi.org/10.1175/2008WAF2222205.1.

Rasmussen, R., and H. Pruppacher, 1982: A wind tunnel and theoretical study of the melting behavior of atmospheric ice particles. I: A wind tunnel study of frozen drops of radius < 500 μm. *J. Atmos. Sci.*, **39**, 152–158, https://doi.org/10.1175/1520-0469(1982)039<0152:AWTATS>2.0.CO;2.

——, and A. Heymsfield, 1987: Melting and shedding of graupel and hail. Part II: Sensitivity study. *J. Atmos. Sci.*, **44**, 2764–2782, https://doi.org/10.1175/1520-0469(1987)044<2764:MASOGA>2.0.CO;2.

Reges, H. W., N. Doesken, J. Turner, N. Newman, A. Bergantino, and Z. Schwalbe, 2016: CoCoRaHS: The evolution and accomplishments of a volunteer rain gauge network. *Bull. Amer. Meteor. Soc.*, **97**, 1831–1846, https://doi.org/10.1175/BAMS-D-14-00213.1.

Rison, W., P. R. Krehbiel, R. J. Thomas, D. Rodeheffer, and B. Fuchs, 2012: The Colorado Lightning Mapping Array. *2012 Fall Meeting*, San Francisco, CA, Amer. Geophys. Union, Abstract AE23B-0319.

Rudlosky, S. D., and H. E. Fuelberg, 2013: Documenting storm severity in the mid-Atlantic region using lightning and radar information. *Mon. Wea. Rev.*, **141**, 3186–3202, https://doi.org/10.1175/MWR-D-12-00287.1.

Ryzhkov, A. V., M. R. Kumjian, S. M. Ganson, and A. P. Khain, 2013a: Polarimetric radar characteristics of melting hail. Part I: Theoretical simulations using spectral microphysical modeling. *J. Appl. Meteor. Climatol.*, **52**, 2849–2870, https://doi.org/10.1175/JAMC-D-13-073.1.

——, ——, ——, and P. Zhang, 2013b: Polarimetric radar characteristics of melting hail. Part II: Practical implications. *J. Appl. Meteor. Climatol.*, **52**, 2871–2886, https://doi.org/10.1175/JAMC-D-13-074.1.

Schlatter, P. T., T. W. Schlatter, and C. A. Knight, 2008: An unusual hailstorm on 24 June 2006 in Boulder, Colorado. Part I: Mesoscale setting and radar features. *Mon. Wea. Rev.*, **136**, 2813–2832, https://doi.org/10.1175/2008MWR2337.1.

Schlatter, T. W., and N. Doesken, 2010: Deep hail: Tracking an elusive phenomenon. *Weatherwise*, **63** (5), 35–41, https://doi.org/10.1080/00431672.2010.503841.

Schultz, C. J., 2015: Physical and dynamical control of lightning jumps and use for assessing severe thunderstorm potential. Ph.D. dissertation, University of Alabama in Huntsville, 208 pp.

——, W. A. Petersen, and L. D. Carey, 2009: Preliminary development and evaluation of lightning jump

algorithms for the real-time detection of severe weather. *J. Appl. Meteor. Climatol.*, **48**, 2543–2563, https://doi.org/10.1175/2009JAMC2237.1.

——, L. D. Carey, E. V. Schultz, and R. J. Blakeslee, 2015: Insight into the kinematic and microphysical processes that control lightning jumps. *Wea. Forecasting*, **30**, 1591–1621, https://doi.org/10.1175/WAF-D-14-00147.1.

Tessendorf, S. A., K. C. Wiens, and S. A. Rutledge, 2007: Radar and lightning observations of the 3 June 2000 electrically inverted storm from STEPS. *Mon. Wea. Rev.*, **135**, 3665–3681, https://doi.org/10.1175/2006MWR1953.1.

van den Heever, S. C., and W. R. Cotton, 2004: The impact of hail size on simulated storms. *J. Atmos. Sci.*, **61**, 1596–1609, https://doi.org/10.1175/1520-0469(2004)061<1596:TIOHSO>2.0.CO;2.

Wallace, R., K. Friedrich, E. Kalina, and P. Schlatter, 2019: Using operational radar to identify deep hail accumulations from thunderstorms. *Wea. Forecasting*, https://doi.org/10.1175/WAF-D-18-0053.1, in press.

Ward, A., M. Kumjian, M. J. Bunkers, S. W. Bieda III, and R. J. Simpson, 2018: Using polarimetric radar data to identify potentially hazardous hail accumulations. *34th Conf. on Environmental Information Processing Technologies*, Austin, TX, Amer. Meteor. Soc., 11B.1, https://ams.confex.com/ams/98Annual/webprogram/Paper326596.html.

Weisman, M. L., and J. B. Klemp, 1982: The dependence of numerically simulated convective storms on vertical wind shear and buoyancy. *Mon. Wea. Rev.*, **110**, 504–520, https://doi.org/10.1175/1520-0493(1982)110<0504:TDONSC>2.0.CO;2.

——, and ——, 1984: The structure and classification of numerically simulated convective storms in directionally varying wind shears. *Mon. Wea. Rev.*, **112**, 2479–2498, https://doi.org/10.1175/1520-0493(1984)112<2479:TSACON>2.0.CO;2.

——, and R. Rotunno, 2000: The use of vertical wind shear versus helicity in interpreting supercell dynamics. *J. Atmos. Sci.*, **57**, 1452–1472, https://doi.org/10.1175/1520-0469(2000)057<1452:TUOVWS>2.0.CO;2.

Wiens, K. C., 2005: Kinematic, microphysical, and electrical structure and evolution of thunderstorms during the Severe Thunderstorm Electrification and Precipitation Study (STEPS). Ph.D. thesis, Colorado State University, 295 pp.

——, S. A. Rutledge, and S. A. Tessendorf, 2005: The 29 June 2000 supercell observed during STEPS. Part II: Lightning and charge structure. *J. Atmos. Sci.*, **62**, 4151–4177, https://doi.org/10.1175/JAS3615.1.

Williams, E. R., and Coauthors, 1999: The behavior of total lightning activity in severe Florida thunderstorms. *Atmos. Res.*, **51**, 245–264, https://doi.org/10.1016/S0169-8095(99)00011-3.

Witt, A., M. D. Eilts, G. J. Stumpf, J. T. Johnson, E. D. Mitchell, and K. W. Thomas, 1998: An enhanced hail detection algorithm for the WSR-88D. *Wea. Forecasting*, **13**, 286–303, https://doi.org/10.1175/1520-0434(1998)013<0286:AEHDAF>2.0.CO;2.

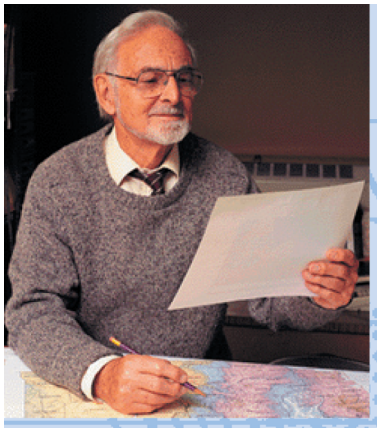

A Half Century of Progress in Meteorology: A Tribute to Richard Reed

edited by Richard H. Johnson and Robert A. Houze Jr.

with selections by: Lance F. Bosart Robert W. Burpee Anthony Hollingsworth James R. Holton Brian J. Hoskins Richard S. Lindzen John S. Perry Erik A. Rasmussen Adrian Simmons Pedro Viterbo

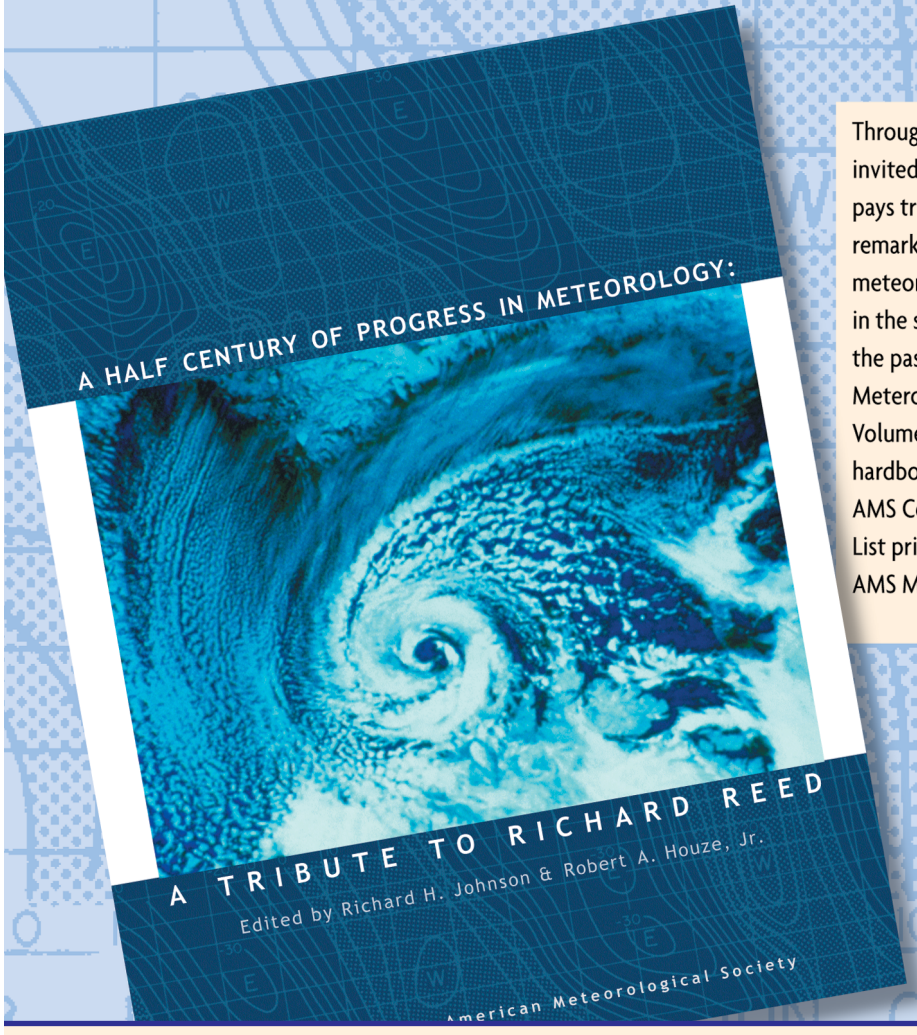

Through a series of reviews by invited experts, this monograph pays tribute to Richard Reed's remarkable contributions to meteorology and his leadership in the science community over the past 50 years. 2003. Meterological Monograph Series, Volume 31, Number 53; 139 pages, hardbound; ISBN 1-878220-58-6; AMS Code MM53.
List price: $80.00
AMS Member price: $60.00

Order Online from bookstore.ametsoc.org